OPEN ACCESS

University of Dundee

# University of Dundee

## Splicing mutation in TAZ gene leading to exon skipping and Barth syndrome

Sivitskaya, Larysa; Danilenko, Nina; Motuk, Iryna; Zhelev, Nikolai

# Splicing mutation in *TAZ* gene leading to exon skipping and Barth syndrome

Larysa Sivitskaya[1], Nina Danilenko[1], Iryna Motuk[2], Nikolai Zhelev[3,4]

[1] Institute of Genetics and Cytology, National Academy of Sciences, Minsk, Belarus; [2] Medical Genetic Department of Regional Perinatal Center, Grodno, Belarus; [3] School of Medicine, University of Dundee, Scotland, UK; [4] Medical University Plovdiv, Bulgaria

**Barth syndrome is a monogenic X-linked disorder characterized by cardiomyopathy, skeletal myopathy and neutropenia. It is caused by deficiency of cardiolipin and associated with mutations in the tafazzin gene (*TAZ*). A 3 years old boy with dilated cardiomyopathy, neutropenia and growth retardation was investigated. Genetic screening found a new variant in the junction of intron 2 and exon 3 of the TAZ gene - c.239-1_239delinsTT. Functional analysis of the variant revealed the aberrant splicing of exon 3 leading to its complete excision from mature mRNA and frameshift at the beginning of tafazzin. Variant c.239-1_239delinsTT can be classified as pathogenic based on splicing alteration and typical clinical phenotype observed in TAZ mutation carriers.**

**Key words:** Barth syndrome, *TAZ*, aberrant splicing, dilated cardiomyopathy, exon skipping

## Introduction

Barth syndrome (BTHS) was originally described in 1983 as an X-linked syndrome of dilated cardiomyopathy, skeletal myopathy and neutropenia causing death in male infancy or early childhood [1]. This syndrome is associated with mutations in the tafazzin (*TAZ*) gene at Xq28 that lead to cardiolipin deficiency and abnormal mitochondria [2,3]. Tafazzin participates in the synthesis of mature cardiolipin (CL) – the necessary component of the mitochondrial membrane, critical for high-energy demand tissues [4]. Lowered tafazzin activity destroys the formation of OXPHOS supercomplexes, mainly in the myocardium tissue and to the cardio-specific loss of the SDH, all these defects lead to the cardiomyopathy [5].

Several phenotypes have been associated with BTHS: dilated cardiomyopathy (most common), left ventricular noncompaction, endocardial fibroelastosis, hypertrophic cardiomyopathy. All these types are associated with the lack or massive suppression of CL synthesis and, as a result, with mitochondrial dysfunction [6].

Neutropenia, another main sign of BTHS, is typically observed in ~ 70% of patients and can be chronic or cyclic and doesn't depend on patient's age [7,8]. It can be more (< 500 cells/mcl) or less (1,000-1,500 cells/mcl) severe; as a result various infections have been reported: recurrent mouth ulcers (4 and more episodes per year), pneumonia, blood infections and others [8].

Muscle weakness – the third sign of the syndrome, is predominantly proximal and non-progressive during childhood. Most boys have more or less delayed gross motor milestones, then in adolescence they are able to walk but often find it hard to kick the ball or to run; up to 18 they usually reach normal height and body mass index [4,9].

We present a clinical report of dilated cardiomyopathy (DCM), neutropenia and skeletal myopathy associated with a *TAZ* splice site mutation in a 3 years old male patient.

## Case presentation

The male patient was born with a weight of 2800 g and a body length of 50 cm. He is the second child in young unrelated parents. Since birth growth retardation (Tab. I) and the motor delay were observed. The boy suffered from increased fatigue, physical intolerance. He showed mild microcytic, hypochromic anemia, cyclic neutropenia with neutrophil 6-18%. There was also a history of infectious illnesses. In the first year of his life, he was treated from acute bronchitis, pneumonia, obstructive bronchitis; in the second year – acute bronchitis, carbuncle of the upper lip. At the age of 3 years 6 months, the boy was admitted to the intensive care unit with lethargy, pallor, puffy face, groaning breathing. Transthoracic echocardiography showed left ventricular dilatation: left ventricle (LV) diameters in end-diastole 38 mm (LVEDD indexed to BSA – 69,1 mm/m$^2$), LV end-diastolic volume index 126ml/m$^2$, LV ejection fraction 39%. Moderate hypertrophy of the LV myocardium, predominantly of the posterior wall was observed. Moderate dilatation of the left atrium (LA) and right atrium (RA) was revealed (LA anterior-posterior and lateral-lateral diameters in the four-chamber 25*28 mm, RA anterior-posterior and lateral-lateral diameters right atrium 22*27 mm), right ventricle (RV) dimension in the four-chamber view was 20*36 mm. Right ventricular function wasn't impaired (Tricuspid Annular Plane Systolic Excursion (TAPSE) – 12 mm). Mitral and tricuspid regurgitation corresponded with II and I degrees. The aortic valve is tricuspid, a function is not impaired. The pulmonary artery pressure is not increased. A small amount of pericardial effusion was detected with separation of pericardial sheets along the anterior wall of

the RA up to 3 mm. Acute myocarditis of unspecified aetiology was diagnosed.

At the age of 4 years, the proband had hypostatura, blonde hair, rounded face, high, wide forehead, deep-set eyes, full cheeks, pointed chin, dimple under the lower lip, slightly protruding large ears. Speech development appropriated for his age. Parents noted the child prefer salty food with spices.

Cytogenetic study of his peripheral lymphocytes showed normal karyotype 46, XY. Tandem mass spectrometry of dry blood spot didn't reveal any significant disturbances.

Clinical examination of family members showed that proband's parents and sister didn't have any cardiac symptoms or abnormal cardiac studies.

## Genetics study

Genomic DNA was obtained from buccal epithelium by phenol/chloroform extraction. We performed the targeted next-generation sequencing (NGS) using the TruSight Cardiomyopathy sequencing kit on the MiSeq System (Illumina Inc., USA). List of 174 genes included in the NGS panel is presented in Table II.

The quality of raw NGS data was estimated with FastQC. The alignment was carried out with BWA against the reference genome NCBIbuild37 (UCSC hg19), the VCF files were generated with a GATK4 HaplotypeCaller. Variants were annotated by ANNOVAR using dbSNP IDs, NHLBI Exome Sequencing Project, The 1000 Genomes Project, the Genome Aggregation Database, ClinVar (2020), InterVar and REVEL. All the variations were classified according to the recommended method of the American College of Medical Genetics and Genomics.

A variant c.239-1_239delinsTT was detected in junction of intron 2 and exon 3 of the *TAZ* gene (NM_000116). It is located in the canonical splice site and predicted to alter splicing according to the Human Splicing Finder. Sanger sequencing confirmed this variant. Segregation analysis revealed that the mutation appeared *de novo*. The patient's mother and sister showed a normal sequence of the *TAZ* gene (Fig. 1).

To confirm the alternative splicing of exon 3, total RNA of the patient and his mother were purified from

**Table I.** Patient's physical development data.

| Age | Weight (g) | Percentiles | Body length (sm) | Percentiles |
|---|---|---|---|---|
| infant | 2800 | 3-10 | 50 | 10-50 |
| 1 year | 7100 | < 3 | 70 | < 3 |
| 2 years 2 months | 9400 | < 3 | 80 | < 3 |
| 3 years 2 months | 10.400 | < 3 | 86 | < 3 |
| 4 years 4 months | 11.900 | < 3 | 92 | < 3 |

**Table II.** List of 174 genes included in the TruSight Cardiomyopathy sequencing kit (from Illumina Inc. USA, mod.).

*ABCC9, ABCG5, ABCG8, ACTA1, ACTA2, ACTC1, ACTN2, AKAP9, ALMS1, ANK2, ANKRD1, APOA4, APOA5, APOB, APOC2, APOE, BAG3, BRAF, CACNA1C, CACNA2D1, CACNB2, CALM1, CALR3, CASQ2, CAV3, CBL, CBS, CETP, COL3A1, COL5A1, COL5A2, COX15, CREB3L3, CRELD1, CRYAB, CSRP3, CTF1, DES, DMD, DNAJC19, DOLK, DPP6, DSC2, DSG2, DSP, DTNA, EFEMP2, ELN, EMD, EYA4, FBN1, FBN2, FHL1, FHL2, FKRP, FKTN, FXN, GAA, GATAD1, GCKR, GJA5, GLA, GPD1L, GPIHBP1, HADHA, HCN4, HFE, HRAS, HSPB8, ILK, JAG1, JPH2, JUP, KCNA5, KCND3, KCNE1, KCNE2, KCNE3, KCNH2, KCNJ2, KCNJ5, KCNJ8, KCNQ1, KLF10, KRAS, LAMA2, LAMA4, LAMP2, LDB3, LDLR, LDLRAP1, LMF1, LMNA, LPL, LTBP2, MAP2K1, MAP2K2, MIB1, MURC, MYBPC3, MYH11, MYH6, MYH7, MYL2, MYL3, MYLK, MYLK2, MYO6, MYOZ2, MYPN, NEXN, NKX2-5, NODAL, NOTCH1, NPPA, NRAS, PCSK9, PDLIM3, PKP2, PLN, PRDM16, PRKAG2, PRKAR1A, PTPN11, RAF1, RANGRF, RBM20, RYR1, RYR2, SALL4, SCN1B, SCN2B, SCN3B, SCN4B, SCN5A, SCO2, SDHA, SEPN1, SGCB, SGCD, SGCG, SHOC2, SLC25A4, SLC2A10, SMAD3, SMAD4, SNTA1, SOS1,SREBF2, TAZ, TBX20, TBX3, TBX5, TCAP, TGFB2, TGFB3, TGFBR1, TGFBR2, TMEM43, TMPO, TNNC1, TNNI3, TNNT2, TPM1, TRDN, TRIM63, TRPM4, TTN, TTR, TXNRD2, VCL, ZBTB17, ZHX3, ZIC3*

whole blood using TRI reagent (Sigma-Aldrich, USA) according to the manufacturer's instructions. Reverse transcription of the total RNA was performed with oligo-dT primers. RT-PCR was carried out with primers specific to exon-exon boundaries in the mature mRNA (transcript variant NM_000116; primer sequences available upon request). The expected size of the amplicons was 249 bp including the exons 1-4. The PCR-fragments were analyzed by electrophoresis in 2% agarose gel, extracted from gel and directly sequenced.

## Results and discussion

We identified new splice variant c.239-1_239delinsTT in *TAZ* gene of the boy with dilated growth retardation. He suffered from cardiomyopathy, cyclic neutrope-

nia and various infections, both local and systemic. We confirmed the alternative splicing of exon 3 due to this variant. RT-PCR analysis showed two different amplicons: 249 bp in healthy mother (corresponds to the wild type) and 204 bp in patient (corresponds to the PCR-product without exon 3). Sequence analysis confirmed the variant c.239-1_239delinsTT led to the skipping of the exon 3 in the mature mRNA (Fig. 2). Thus the genetic reason for DCM in our patient was the complete excision of exon 3 causing a frameshift at the beginning of tafazzin.

To date, 12 splicing mutations in the *TAZ* gene have been reported in ClinVar as pathogenic or likely pathogenic. Several of them were found in the junction of intron 2 and exon 3 of the *TAZ* gene. Probably all of them result in the aberrant splicing of exon 3, but the functional analysis has been conducted for few. Interestingly, other
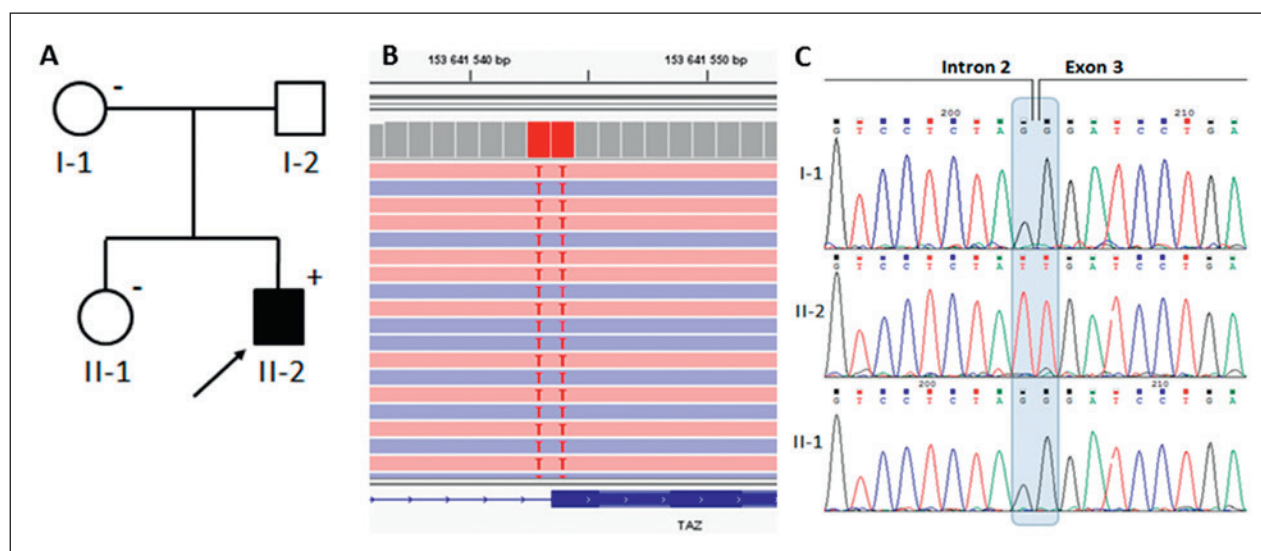


**Figure 1.** A) Pedigree of the studied family. The solid symbol indicates clinically affected subjects. The arrow denotes the proband. Symbols (+) and (-) indicate *TAZ* mutation carriers and non-carriers in X-chromosome, respectively. The absence of a symbol denotes that genetic analysis was not performed; B) NGS reads detecting mutation in intron-exon junction; C) Electrophoregram showing the DNA sequence for the junction of intron 2 and exon 3 in *TAZ* gene.
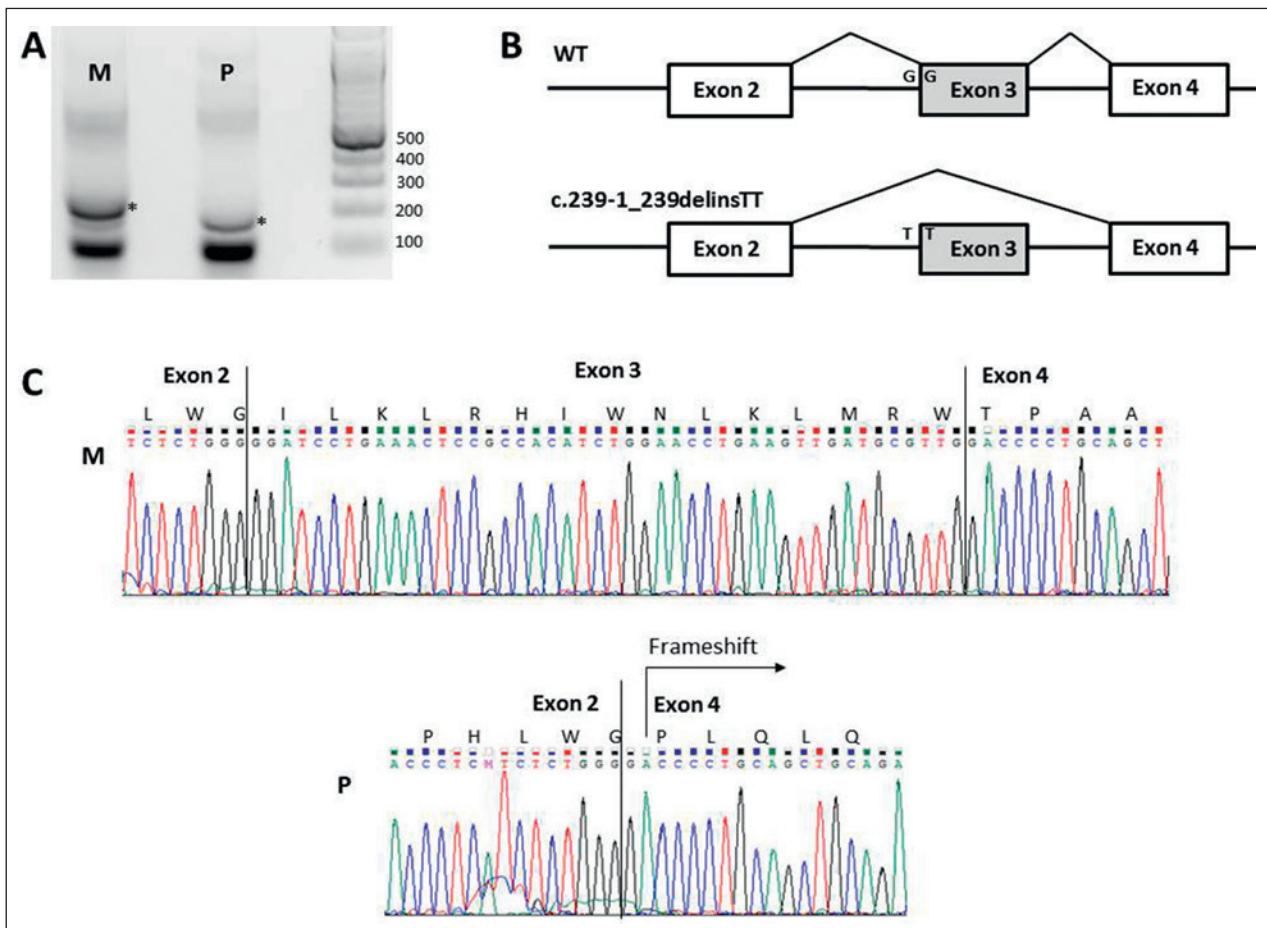
**Figure 2.** A) Electrophoretic analysis of the RT-PCR products. P – proband, M – mother. The asterisks indicate bands extracted from gel and sequenced. The smaller PCR-product (204 bp) in agarose gel electrophoresis corresponds to a transcript without exon 3; B) *TAZ* gene diagram showing mutation location and its effect on splicing; C) Sequence analysis of RT-PCR products from the proband (P) and mother (M) revealed skipping of exon 3 in proband.

effects on splicing were shown for the base changes identified in the same locus - c.239-1G>C and c.239-1G>A. The first one abolishes splicing of intron 2, the second one reconstitutes the splice site with a 1 base shift [3]. In any case, the mutations interfere with the translation of tafazzin and result in BTHS.

Mutations causing BTHS are of several types including splice site mutations, frameshifts, insertions, deletions, nonsense, and missense mutations. They lead to decreased or missing tafazzin enzymatic activity, with correspondingly more or less global changes in cardiolipin content and composition associated with the disease severity. Unfortunately, not for all TAZ gene mutations the correlation between genotype and phenotype is apparent [10].

Whited et al. (2013) developed and applied a BTHS-mutant panel in the yeast *Saccharomyces cerevisiae*. The authors introduced disease-causing variants into the Taz1p yeast ortholog to investigate loss-of-function

mechanisms of tafazzin. As a result, seven functional classes of BTHS mutations were defined: (1) non-functional proteins resulted from frameshifts and splice-site variants, (2) submitochondrial mislocalization and erroneous aggregation of products, (3) altered assembly of tafazzin, (4) catalytically inactive proteins, (5) low expression of tafazzin, (6) products unable to engage in stable productive assemblies (7) temperature-sensitive proteins [11]. The processes of cardiolipin biosynthesis and remodeling are conserved from yeast to humans and therefore identified mechanisms bring us closer to the understanding of the genetic basis and clinical variability of BTHS. Later some of these functional classes were documented in human tafazzin within human cells [12].

In conclusion, this is the first description of c.239-1_239delinsTT variant causing the Barth syndrome. This splice-site variant can be considered as pathogenic for the following reasons: abnormal splicing

of the *TAZ* leading to the skipping of the exon 3 (PVS1), *de novo* variant in the family without a history of DCM or heart failure (PS2), typical clinical phenotype observed in *TAZ* mutation carriers (PP4), absence in population databases Exome Sequencing Project, 1000 Genomes Project and Exome Aggregation Consortium (PM2).

*Conflict of interest*

The Authors declare no conflict of interest.

*Author contributions*

LS, ND and NZ conceived and planned the research. IM and LS carried out the clinical and genetic analysis. NZ contributed to the interpretation of the results. LS wrote the manuscript with support from ND and IM.

## References

1    Barth PG, Scholte HR, Berden JA, et al. An X-linked mitochondrial disease affecting cardiac muscle, skeletal muscle and neutrophil leucocytes. J Neurol Sci 1983;62:327-355. https://doi.org/10.1016/0022-510X(83)90209-5

2    Barth PG, Van den Bogert C, Bolhuis PA, et al. X-linked cardioskeletal myopathy and neutropenia (Barth syndrome): respiratory-chain abnormalities in cultured fibroblasts. J Inherit Metab Dis 1996;19:157-160. https://doi.org/10.1007/BF01799418

3    Bione S, D'Adamo P, Maestrini E, et al. A novel X-linked gene, G4.5. is responsible for Barth syndrome. Nat Genet 1996;12:385-389. https://doi.org/10.1038/ng0496-385

4    Finsterer J. Barth syndrome: mechanisms and management. Appl Clin Genet 2019;12:95-106. https://doi.org/10.2147/TACG.S171481

5    Dudek J, Cheng IF, Chowdhury A, et al. Cardiac-specific succinate dehydrogenase deficiency in Barth syndrome. EMBO Mol Med 2016;8:139-154. https://doi.org/10.15252/emmm.201505644

6    Sabbah HN. Barth syndrome cardiomyopathy: targeting the mitochondria with elamipretide. Heart Fail Rev 2021;26:237-253. https://doi.org/10.1007/s10741-020-10031-3

7    Folsi V, Miglietti N, Lombardi A, et al. Cardiomyopathy in a male patient with neutropenia and growth delay. Ital J Pediatr 2014;40:45. https://doi.org/10.1186/1824-7288-40-45

8    Roberts AE, Nixon C, Steward CG, et al. The Barth syndrome registry: distinguishing disease Characteristics and growth data from a longitudinal study. Am J Med Genet A 2012;158A:2726-2732. https://doi.org/10.1002/ajmg.a.35609

9    Clarke SL, Bowron A, Gonzalez IL, et al. Barth syndrome. Orphanet J Rare Dis 2013;8:23. https://doi.org/10.1186/1750-1172-8-23

10   Ronvelia D, Greenwood J, Platt J, et al. Intrafamilial variability for novel TAZ gene mutation: Barth syndrome with dilated cardiomyopathy and heart failure in an infant and left ventricular noncompaction in his great-uncle. Mol Genet Metab 2012;107:428-432.

11   Whited K, Baile MG, Currier P, et al. Seven functional classes of Barth syndrome mutation. Hum Mol Genet 2013;22:483-492. https://doi.org/10.1093/hmg/dds447. Epub 2012 Oct 24. PMID: 23100323; PMCID: PMC3606006.

12   Lu YW, Galbraith L, Herndon JD, et al. Defining functional classes of Barth syndrome mutation in humans. Hum Mol Genet 2016;25:1754-1770.